Available online at www.sciencedirect.com
SCIENCE DIRECT
Carbohydrate Polymers 58 (2004) 15–24
Carbohydrate Polymers
www.elsevier.com/locate/carbpol

Rheological properties of gellan, κ-carrageenan and alginate polysaccharides: effect of potassium and calcium ions on macrostructure assemblages

M.T. Nickerson, A.T. Paulson*

Department of Food Science and Technology, Dalhousie University, P.O. Box 1000, Halifax, NS, Canada B3J 2X4

Received 19 November 2003; revised 15 June 2004; accepted 17 June 2004
Available online 10 August 2004

Abstract

The effect of added ions (0.5 mM K^+ or 0.25 mM Ca^{2+}) on the critical overlap (C^*) and gelation (C_o') concentrations for gellan, κ-carrageenan and alginate polysaccharides were investigated using steady shear rheometry. Both C^* and C_o' decreased for all solutions with added salts, a trend more pronounced for gellan and alginate with added Ca^{2+}, and κ-carrageenan with added K^+. Aggregation near the sol–gel transition was modeled as a percolation-type transition. In addition, the frequency dependence of the viscoelastic storage (G') and loss (G'') moduli for bulk and localized areas within a 0.7% (w/w) gellan sol were measured using a controlled stress and oscillating magnetic bead rheometer, respectively. Flow behavior of the bulk was in the terminal and plateau relaxation regions of the viscoelastic spectrum, whereas localized behavior was in the plateau and rubber–glass transition regions.

Keywords: Gellan; Alginate; Carrageenan; Percolation; Aggregation; Critical overlap concentration and gelation

1. Introduction

The behavior of polysaccharides near the sol–gel transition changes dramatically with polymer and counter-ion concentration. Beyond the dilute concentration regime, chain overlap, entanglement and formation of ion-mediated junction zones increase as intermolecular interactions become more frequent, leading to the formation of macrostructure assemblages or aggregates (Jampen, Britt, & Tung, 2000). The concentration at which chain overlap is first detected is deemed the critical overlap concentration (C^*), and is considered the upper limit of dilute solution behavior (Harding, 1998). Experimentally, C^* is evident by a notable rise in viscosity with increasing polymer concentration as solutions change from Newtonian to a non-Newtonian fluid, as measured by steady shear rheometry (Ferry, 1980). A three-dimensional network or gel is formed once the polymer concentration reaches the critical gelation concentration (C_o'). At C_o', zero shear viscosity (η_o') diverges to infinity indicating that the diffusion of individual chains or assemblages effectively ceases due to the formation of a gel (Arbabi & Sahimi, 1990; Borchard & Lechtenfeld, 2001; Broderix, Löwe, Müller, & Zippelius, 2000; Del Gado, de Arcangelus, & Coniglio, 2002). Although the entanglement of polysaccharide chains usually occurs during gelation, C^* may be greater than C_o', since the former is molecular weight dependent whereas the latter may not be (Morris, 1998). Investigation of the mechanisms driving chain aggregation during gelation will allow for better control for their use as food ingredients in both weak and strong gel systems.

In the present study, the effect of K^+ and Ca^{2+} on the rheological properties of de-acyl gellan, κ-carrageenan and alginate solutions near the sol–gel transition were investigated with steady and oscillatory shear rheometry. All three polysaccharides are proposed to have an overall similar mode of aggregation, but differ with respect to their ion-mediated junction zones. De-acyl gellan is a linear exocellular polysaccharide, secreted from the bacterium

* Corresponding author. Fax: +1-902-420-0219.
E-mail address: allan.paulson@dal.ca (A.T. Paulson).

0144-8617/$ - see front matter © 2004 Elsevier Ltd. All rights reserved.
doi:10.1016/j.carbpol.2004.06.016

Sphingomonas elodea (ATCC 31461), and consists of repeating tetrasaccharide units of [→3)-β-D-glucose-1→4)-β-D-glucuronic acid-(1→4)-β-D-glucose-(1→4)-α-L-rhamnose-(1→]$_n$ (Jansson, Lindberg, & Sandford, 1983; Robinson, Manning, & Morris, 1991). Gellan forms Ca^{2+}-mediated junction zones by cross-linking two double helices (Chandrasekaran & Radha, 1995; Chandrasekaran, Radha, & Thailambal, 1992). In contrast, κ-carrageenan is a linear sulfated polysaccharide extracted from red seaweed (*Rhodophyceae*), and consists of repeating disaccharide units of alternating (1→3)-α-D-galactose-4-sulphate and (1→4)-β-3,6-anhydro-D-galactose residues (Harding, Day, Dhami, & Lowe, 1997; Lahaye, 2001; Thành, Yuguchi, Mimura, Yasunaga, Takano, Urkawa, et al. 2002; Ueda, Itoh, Matsuzaki, Ochiai, & Imamura, 1998). Kappa-carrageenan forms K^+-mediated junction zones of multi-stacked single (Smidsrød & Grasdalen, 1982) or double (Anderson, Campbell, Harding, Rees, & Samuel, 1969) helices. Alternatively, alginate is a linear polyuronic polysaccharide extracted from brown seaweed (Phaeophyceae), and consists of (1→4)-linked blocks of poly-β-D-mannuronic acid (M), poly-α-L-guluronic acid (G) and mixed MG blocks. Junction zones for alginate are considered to be Ca^{2+}-mediated, multi-stacked buckled ribbons that resemble 'egg box-like' structures (Lahaye, 2001; Morris, 1986, 1998).

Controversy arises over the mode of aggregation, whether chains associate into filaments (fibril model) or individual clusters (domain model). The former model suggests that during aggregation ordered structures align end-to-end to form a filament, which becomes thicker with increasing salt and polymer concentrations (Morris, 1995, 1998). The latter model suggests chains associate as individual ion-mediated clusters or aggregates which become entangled with other clusters until forming an infinite cluster or gel (Morris, Rees, & Robinson, 1980; Robinson et al., 1991). This controversy may be resolved by studying the scaling properties of viscosity and gel elasticity at concentrations below and above C_o', respectively, using either a percolation model (de Gennes, 1979; Ikeda, Tokita, Tsutsumi, & Hikichi, 1989; Tempel, Isenburg, & Sachmann, 1996; Yano, Kumagai, Fujii, & Inukai, 1993) or a classical tree-like approximation (de Gennes, 1979). The percolation model considers aggregates as square lattices, where each point represents a reactive group along the polysaccharide backbone (de Gennes, 1979; Stauffer, Coniglio, & Adam, 1982; Yano et al., 1993). The probability of finding a reactive site is denoted by P_s. Each site has a probability of forming a bridge between adjacent chains, denoted as P_b. If one of either P_s or P_b is fixed, then the other will increase to some critical probability, P_c, of which an infinite size cluster exists (analogous to a three-dimensional gel) (Ikeda et al., 1989; Stauffer et al., 1982; Yano et al.). If $P_b < P_c$, then small clusters exist, whereas if $P_b > P_c$ than an infinite cluster is formed (de Gennes, 1979; Stauffer et al., 1982). In practice, P_c and P_b are substituted with C_o' and C (polymer concentration), respectively.

The scaling laws for the percolation theory are given by (Yano et al., 1993):

$$\eta_o' = A_1(C_o' - C)^{-s} \quad (1)$$

$$G_o' = A_2(C - C_o')^t \quad (2)$$

where η_o', zero shear viscosity; G_o', dynamic storage modulus at zero frequency; A_1 and A_2, constants; and s and t are critical scaling exponents that theoretically range between 0.7–1.3 and 1.7–2.0, respectively, for the site-bonded percolation model (Borchard & Lechtenfeld, 2001; Del Gado et al., 2002; Yano et al., 1993). The scaling behavior of η_o' and G_o' can also be related to the classical tree-like approximation, which describes growing clusters as branches, capable of diverging at any site along the chain and assumes that neighboring branches do not interfere with others (de Gennes, 1979). This approximation estimates critical exponents, s and t, to be 0 and 3, respectively (Borchard & Lechtenfeld, 2001; Stauffer et al., 1982). However, this theory gives a gross simplification of aggregation since it fails to include excluded volume effects, assumes that no steric hindrance occurs between neighboring chains and neglects intermolecular loops (i.e. cyclic bonds) (Borchard & Lechtenfeld, 2001; Stauffer et al., 1982). In the present study, aggregation by the domain and fibril models is analogous to the percolation model and classical tree-like approximation, respectively.

The viscoelastic behavior of an entangled gellan solution was also investigated using a controlled stress and oscillating magnetic bead rheometer. The former rheometer makes averages of the viscoelastic behavior over the bulk, neglecting local thermal fluctuations and inhomogeneities that are integral components of the gel network, whereas the latter rheometer measures local areas within the sample to give viscoelastic information about the microstructure (Ziemann, Rädler, & Sackmann, 1994).

2. Materials and methods

2.1. Materials

De-acyl gellan powder (Kelcogel F, lot# 1D0608A, 2002) (CP Kelco, San Diego, CA) consisted of 88.66% (w/w) gellan, 7.0% (w/w) water and minute amounts of calcium (0.39% w/w), sodium (0.44% w/w), magnesium (0.087% w/w), potassium (3.38% w/w) (atomic adsorption) and phosphorus (0.041% w/w) (colorimetric analysis). Kappa-carrageenan powder (Genugel carrageenan, type CHP-2F, lot# 93756, 1999) (CP Kelco, San Diego, CA) consisted of 77.47% (w/w) polymer, 14.35% (w/w) potassium, 7.3% (w/w) water, and small amounts of calcium (0.12% w/w), sodium (0.64% w/w), magnesium

(0.12% w/w) (atomic adsorption) and phosphorus (0.002% w/w) (colorimetric analysis). Alginate powder (Protanal GP 9356, lot# S12748, 2001) (FMC Biopolymer, Drammen, Norway) consisted of 85.47% (w/w) polymer, 13.18% (w/w) sodium, 8% (w/w) water, and small amounts of calcium 1.17% (w/w), potassium (0.17% w/w), magnesium (0.002% w/w) (atomic adsorption) and phosphorus (0.011% w/w) (colorimetric analysis). The polymer content, in all cases was determined by the difference of the sum of the water and ionic constituents from 100%, assuming the differential weight represented the pure polymer species. It should be noted that impurities within the powder and the polymer itself may occur, however, are considered negligible. Powders were used without further purification. Salt stock solutions were prepared in distilled de-ionized water (DDW) using 1 M $CaCl_2 \cdot 2H_20$ and KCl.

2.2. Steady shear rheometry

Polysaccharide powders were dispersed in DDW using a magnetic stirrer at room temperature. The dispersions were heated to 100 °C and allowed to boil vigorously for 10 min with continuous stirring. The sol was allowed to cool to room temperature, prior to correcting for evaporative losses by the addition of DDW. Various volumes of sample were transferred into 15 ml capped plastic centrifuge tubes, followed by dilutions with DDW to obtain a wide concentration range. Potassium or Ca^{2+} was added directly from a stock solution, and thoroughly mixed.

The apparent viscosity (η) was determined with a Bohlin controlled stress (CS10) rheometer (Bohlin Inc., Cranbury, NJ). Solutions were poured into a concentric cylinder fixture (C25) at 25 °C and allowed to equilibrate for 5 min. A thin layer of mineral oil was applied on top of the submerged bob to prevent evaporative losses. A shear rate sweep was performed, by ramping the shear rate both in the upward and downward directions over a range of 24.1–201.6 s^{-1}. All samples were measured in duplicate. No hysteresis was evident between upward and downward sweeps over this shear rate range, indicating no time dependencies over the time scale of the experiment (Tung & Paulson, 1995). As a result, data from both the upward and downward sweeps were pooled. Polysaccharide solutions in the absence and presence of added K^+ (0.5 mM) or Ca^{2+} (0.25 mM) were measured. Polysaccharide concentrations ranged from 0.075 to 0.6% (w/w) depending on the polymer-type and counter-ions present.

The critical overlap concentration was determined by plotting specific viscosity (η_{sp}) vs. concentration on logarithmic axes as described by Jampen et al. (2000). The specific viscosity was determined by $(\eta/\eta_{solv})-1$, where η_{solv} is the solvent viscosity which was equivalent to 0.893 mPa s (Weast, 1975). The inflection point was taken to be indicative of C^*, as determined by linear piecewise regression (SPSS Inc., Ver. 5.0, 1994, Chicago, IL), which searched for the two lines of best fit through the data. The η_{sp} was arbitrarily selected at 49 s^{-1}, where below C^* under steady shear conditions, solutions behaved as Newtonian fluids; above C^*, solutions become non-Newtonian and shear rate-dependent (Ferry, 1980). Rheograms for gellan solutions (no added salts) below and above C^* are shown in Fig. 1a, as a representative sample. Flow properties were described by the power-law model:

$$\sigma = m\dot{\gamma}^n \tag{3}$$

where $\dot{\gamma}$, shear rate (s^{-1}); σ, shear stress (Pa); m, consistency coefficient; n, flow behavior index. The latter distinguishes whether the solution behaves as a Newtonian ($n=1$) or non-Newtonian liquid ($n<1$ for our samples). Fig. 1b plots the flow behavior index as a function of concentration, to confirm Newtonian behavior below C^* and non-Newtonian behavior afterwards.

The critical gelation concentration and scaling exponent were determined as described by Yano et al. (1993) using viscosity data only, since G' was below the sensitivity of the rheometer. A representative example of this method is depicted in Section 3.2 (Fig. 3) for a gellan solution in the absence of added salts. The critical gelation

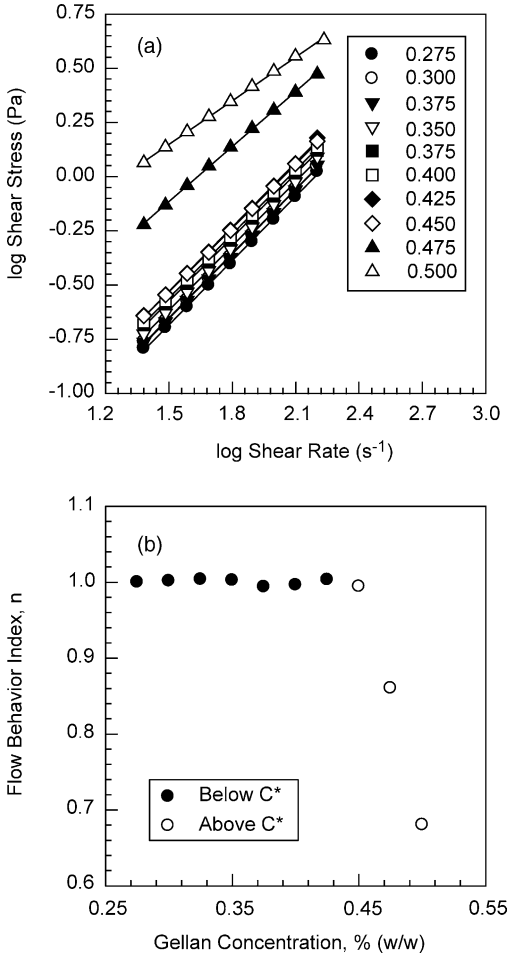

Fig. 1. Rheograms fitted to the power-law model (a) and the flow behavior indices (b), both as a function of polymer concentration for gellan solutions in the absence of added ions at 25 °C.

concentration as a function of shear rate (24.1, 38.7, 62.1, 99.7 and 160.0 s^{-1}) was determined in a plot of $1/\eta$ vs. concentration (C), and fitted with linear regression. As C approaches C_o, η increases to infinity and $1/\eta$ approaches zero. The shear rate-dependent C_o was then determined by extrapolating the linear regression lines to the concentration axis where $1/\eta$ was made to equal zero. The critical overlap concentration at zero shear (C_o') was estimated by plotting C_o vs. shear rate, followed by linear regression and extrapolation to zero shear. The critical scaling exponent, s, was then determined from the slope of η vs. $(C_o' - C)$ plots on logarithmic axes as a function of shear rate. The critical scaling exponent at zero shear (s') was then estimated by extrapolating a linear regression line in a plot of s vs. shear rate to zero shear.

The effects of polymer-type and salts on C^*, C_o' and s' were analyzed using Systat software (SPSS Inc., Ver. 10, 2000, Chicago, IL) by an individual degree of freedom (orthogonal) contrast analysis using the general linear model (Li, 1964). This analysis is an extension of a conventional analysis of variance (ANOVA) because it allows specific predetermined treatment contrasts, each with 1 degree of freedom, to be tested rather than less specific overall treatment and interaction effects. The effect of salts (K^+ and Ca^{2+}) vs. no salts, K^+ vs. Ca^{2+}, polymer ((A) gellan and alginate vs. κ-carrageenan and (B) gellan vs. alginate) and associated interactions (i.e. (1) no salts vs. salts × polymer A or B and (2) K^+ vs. Ca^{2+} × polymer A or B) were used as the individual degree of freedom contrasts. Gellan and alginate were differentiated from κ-carrageenan in polymer A because both contain carboxyl groups, whereas κ-carrageenan has a sulfate group.

2.3. Oscillatory shear rheometry

The dynamic storage (G') and loss (G'') moduli were measured for a 0.7% (w/w) gellan solution over a frequency range of 0.08–10 Hz, and a maximum strain amplitude of 2% with a Bohlin controlled stress (CS10) rheometer. The gellan sample was prepared in a similar manner as Section 2.2. The gellan sol was poured into a concentric cylinder fixture (C25) at 25 °C and allowed to equilibrate for 10 min. A thin layer of mineral oil was applied on top of the submerged bob to prevent evaporative losses. All measurements were made within the linear viscoelastic region. The average length scale probed by this fixture was 50 μm, as determined by multiplying the maximum stain amplitude (0.02) by the width of the fixture's gap (2.5 mm) (Steffe, 1996).

Localized viscoelastic behavior within the bulk was measured with a custom-built oscillating magnetic bead rheometer in the Biophysics Department at the Technical University of Munich (Technische Universität München). Instrument specifications and derivation calculations for viscoelastic moduli from an oscillating force are described by Keller, Schilling, and Sackmann (2001). To summarize, the rheometer consists of two electromagnetic coils with soft iron cores, mounted onto the stage of a Zeiss Axiovert microscope. A cuvette containing the gellan sample with embedded magnetic beads was placed between the two coils. An inhomogeneous magnetic field is induced by the coils proportional to the current applied, producing a corresponding force that causes the beads to oscillate. This force–current relationship is calibrated using a known viscosity glycerol–salt–water mixture and Stokes' law ($f_o = 6\pi R\eta x$, where R is the bead radius and x denotes particle speed). Bead position in the xy plane is tracked by video images over time, which is then digitized by a computer equipped with a pixel-pipeline frame-grabber card and fitted by two-dimensional Fast Fourier Transform analysis. The frequency of the oscillating beads is described by a sinusoidal wave function. The amplitude, $x_o(\omega)$ and the phase shift, $\phi(\omega)$ of this wave are then used in the following equations to derive viscoelastic functions:

$$G'(\omega) = [f_o/(6\pi R|x_o(\omega)|)] \times \cos\varphi(\omega) \quad (4)$$

$$G''(\omega) = [f_o/(6\pi R|x_o(\omega)|)] \times \sin\varphi(\omega) \quad (5)$$

where f_o is the force acting on the bead (Ziemann et al., 1994). In the present study, 2 μl of spherical superparamagnetic Dynabeads M-450 (4.5 μm diameter, density 10^5 beads/ml, Deutsche Dynal, Hamburg, DEU) were vortexed with 1 ml of a 0.7% (w/w) gellan solution cooled to 25 °C. The gellan–bead mixture (15 μl) was pipette into the cuvette, where it equilibrated for 10 min to allow structures to re-form. Frequency sweeps (0.08–15.1 Hz) were performed on four separate beads embedded within the same gellan matrix using a constant magnetic force of 2.55 pN at 25 °C. Strain amplitude for an oscillating bead was varied between 120 and 7.38 nm corresponding to the low (0.08 Hz) and high (15.1 Hz) ends of the frequency spectrum, respectively. The average distance between embedded beads was 100 μm. The applied force was calibrated against coil current according to Keller et al. (2001) using an oscillating bead suspended in a glycerol–water–salt solution (0.4 g/g water, 0.1 g/g glycerol, 0.5 g/g $CsCl_2$), giving a linear force–current calibration curve.

3. Results and discussion

3.1. Critical overlap concentration

Using steady shear rheometry, C^* was apparent as an inflection point in a double logarithmic plot of η_{sp} as a function of polysaccharide concentration, as shown in Fig. 2a for a gellan solution in the absence of added ions at 25 °C. Similar plots were observed for other gellan solutions and for κ-carrageenan and alginate polysaccharides in the absence and presence of added ions. Mean C^* values for all solutions are shown in Fig. 2b. An individual degree of freedom contrast analysis found that all main effects and all interactions but one were significant ($P < 0.001$, Table 1).

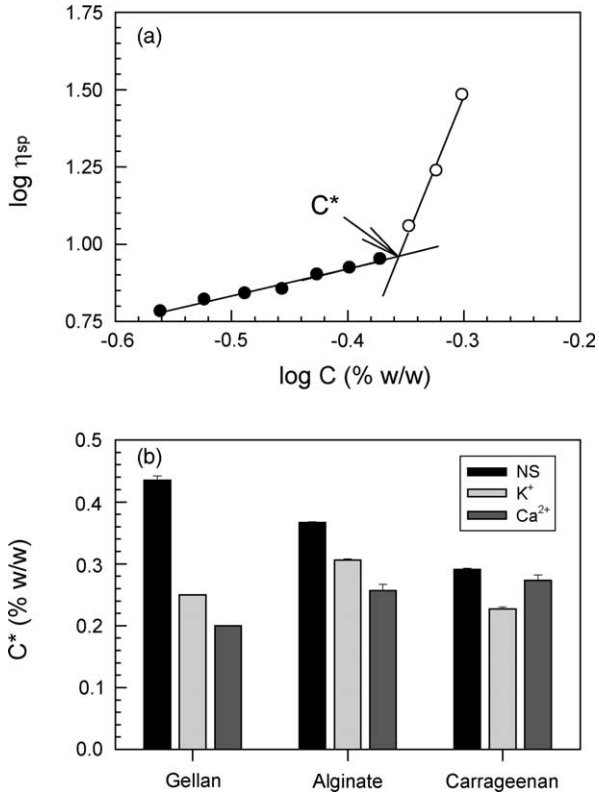

Fig. 2. The critical overlap concentration (C^*) for a gellan solution in the absence of added ions at 25 °C, as determined by the use of linear piecewise regression analysis of the specific viscosity at 49.1 s^{-1} as a function of polymer concentration (C) (a). The critical overlap concentration as a function of polymer-type (i.e. gellan, alginate or κ-carrageenan) for solutions in the absence (NS) and presence of 0.5 mM K^+ or 0.25 mM Ca^{2+} ($n=2$). Error bars represent one standard deviation (b).

Table 1
An individual degree of freedom (orthogonal) contrast analysis for dilute polymer solutions ($n=18$)

Conditions	Critical overlap concentration (C^*)	Critical gelation concentration (C_o')	Percolation scaling exponent at zero shear (s')
Main effects			
No salts vs. salts	$P<0.001$	$P<0.001$	NS
K^+ vs. Ca^{2+}	$P<0.001$	NS	NS
Polymer A (gellan/alginate vs. κ-carrageenan)	$P<0.001$	$P<0.05$	NS
Polymer B (gellan vs. alginate)	$P<0.001$	$P<0.001$	NS
Interactions			
Polymer A × no salts vs. salts	$P<0.001$	$P<0.001$	NS
Polymer A × K^+ vs. Ca^{2+}	$P<0.001$	$P<0.001$	NS
Polymer B × no salts vs. salts	$P<0.001$	$P<0.001$	NS
Polymer B × K^+ vs. Ca^{2+}	NS	$P<0.05$	NS

NS, not significant ($P>0.05$); all contrasts have one degree of freedom.

The presence of significant interactions means that generalizations regarding the main effects must be made with caution, since the effect of one treatment (type of polymer) depends upon the other (type of salt). Overall, the critical overlap concentration was lower in the presence of salts, but the effect of salt was different for each polymer. The significant interactions between polymer contrast A (i.e. gellan/alginate vs. κ-carrageenan) and the salt contrasts (i.e. (1) no salts vs. salts or (2) K^+ vs. Ca^{2+}) suggest that the effects of salts are different between polymers whose reactive groups are carboxyl (gellan; alginate) than those with sulfate groups (κ-carrageenan). Overall, the main contrasts: polymer A, no salts vs. salts and K^+ vs. Ca^{2+} were significant ($P<0.001$, Table 1). All polymers had lower C^* values in the presence of added salts than without. However, κ-carrageenan solutions in the absence of added salts and with added Ca^{2+} had similar C^* values (Fig. 2b). The critical overlap concentration for gellan and alginate decreased further with added Ca^{2+} than K^+, whereas the opposite was true for κ-carrageenan. The interaction between polymer B (i.e. gellan vs. alginate) and the no salts vs. salts contrast was also significant ($P<0.001$), however, the interaction between polymer B and the K^+ vs. Ca^{2+} contrast was not ($P>0.05$, Table 1). Both polymers in the presence of salts had lower C^* values than solutions without ($P<0.001$), although C^* for gellan decreased further than with alginate.

Gellan in the presence of Ca^{2+} had the lowest C^*, attributed to a combination of charge screening and ion-mediated cross-linking between double helices, which then lead to the formation of larger aggregates. Consequently, chain overlap is detected at lower concentrations. Jampen et al. (2000) reported C^* for Na^+–gellan to be 0.064% (w/v). Watase and Nishinari (1993) and Nickerson, Paulson, and Speers (2003) found C^* for gellan solutions to decrease with the addition of cations. Tang, Tung, and Zheng, (1997a,b) developed a mathematical model to predict the number of divalent cations involved in cross-linking four gellan polymers. Mao, Tang, and Swanson (1999) and Nickerson et al. (2003) estimated that 3 Ca^{2+} ions were involved in cross-linking four gellan chains using the sol–gel transition temperatures and C^* values at different temperatures, respectively.

The exact mechanism of interaction between K^+ ions and gellan chains is unknown. However, the ion–water bridge ($-K^+\cdots H_2O\cdots K^+-$) proposed by Chandrasekaran et al. (1992) may not be the only mechanism involved because the addition of monovalent ions requires ~25–40 times the ionic strength as divalent ions to obtain comparable gel rigidities (Doner & Douds, 1995; Sanderson & Clark, 1983; Tang, Tung, & Zeng, 1995; Tang et al., 1997a). In the present study, it is proposed that the addition of K^+ reduces intermolecular charge repulsion between adjacent helical domains through charge screening to allow for closer associations promoting intermolecular interactions. According to the DLVO theory, the presence of ions reduces

the thickness of the electric double layer and the energy needed to overcome the repulsive barrier at intermediate chain separation distances to allow van der Waals attractive forces to predominate (Narsimhan, 1992). It is hypothesized that these associations are further stabilized by hydrogen bonding and by the ion–water bridge. Since there is a greater amount of polymer–polymer interactions relative to gellan samples without salts, larger macrostructure assemblages form giving a lower C^*. The large differences in gel rigidity reported between gellan gels with K^+ and Ca^{2+} stem from ion-specific polymer interactions. Calcium ions form semi-crystalline ion-mediated junction zones (i.e. thermally stable ionic bridges) between neighboring carboxyl sites. In addition, divalent ions are much better at screening charged sites than monovalent ions. According to the Schultze-Hardy rule the effectiveness of screening charged sites is proportional to the sixth power of the counterion valency number (Narsimhan, 1992). Consequently, much more monovalent ions are required to obtain similar gel rigidities than if divalent ions were present.

The critical overlap concentration for κ-carrageenan solutions decreased with the addition of salts relative to solutions without, and decreased further with added K^+ than Ca^{2+}. It is proposed that in the present study, the addition of K^+ promotes the formation of larger aggregates than with other treatments due to enhanced chain stability caused by increased charge screening and ion-mediated attractive forces. te Nijenhuis (1997) proposed that K^+ forms an ionic bond with the sulfate group from one galactose residue and an electrostatic interaction with an anhydro-O-3,6-ring of another galactose residue to stabilize intermolecular associations between adjacent double or single helices. In contrast, Ca^{2+} is proposed to cross-link sulfate groups on neighboring single or double helices and participate in charge screening. Larger macrostructure assemblages lead to a lower C^*. Meunier, Nicolai, and Durand (2000) reported the parallel stacking of multiple κ-carrageenan chains within aggregates. Morris et al. (1980) estimated stacked junction zones to consist, on average, of 10 chains, based on the molecular weights of both coils and aggregates. Croguennoc, Meunier, Durand, and Nicolai (2000) estimated C^* for κ-carrageenan solutions at 0.11% (w/w), which is approximately half of that found in the present study. However, C^* is affected by polymer size, ionic strength and carrageenan structure, therefore discrepancies in reported values are expected.

For alginate solutions, C^* decreased with added salts relative to solutions without, and decreased further with added Ca^{2+} than K^+ (Fig. 2b). It is proposed that K^+ screens carboxyl groups along the alginate backbone, reducing intermolecular charge repulsion between chains to promote closer associations. This is proposed to lead to

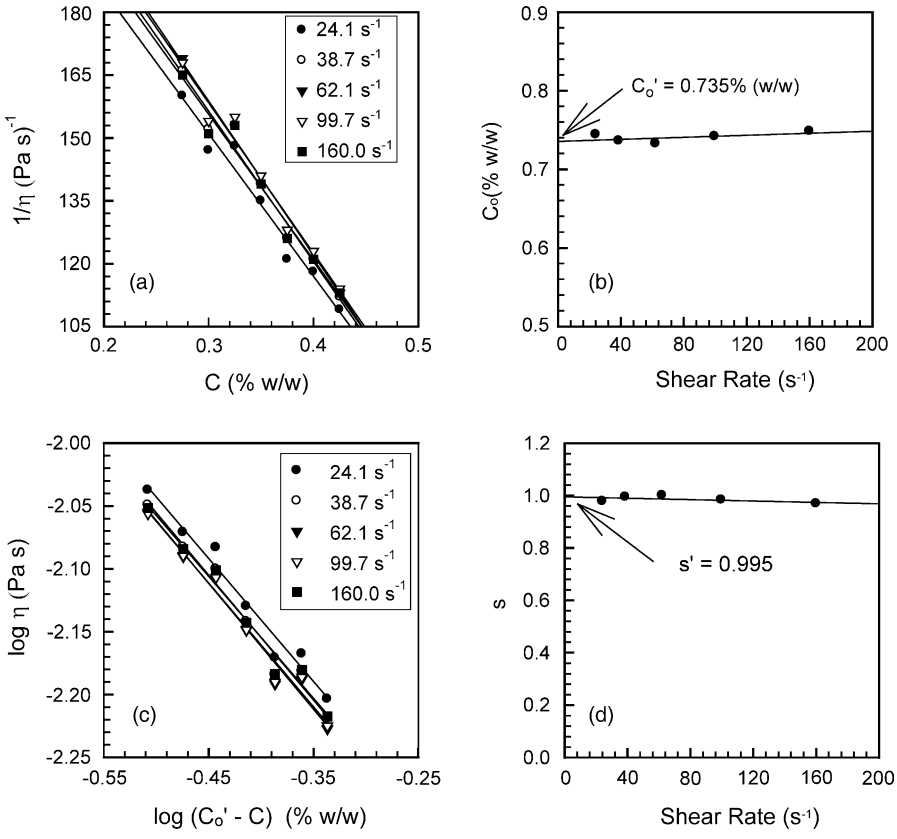

Fig. 3. The percolation theory applied to a gellan solution in the absence of added counterions, where (a) represents the dependence of inverse viscosity (η) on concentration (C), (b) describes the shear rate dependence of the critical gelation concentration (C_o), (c) gives a double logarithmic plot of η vs. the concentration difference ($C_o' - C$) and (d) describes the shear rate dependence of the critical scaling exponent (s).

larger macromolecular assemblages being formed and a lower C^*. In the presence of Ca^{2+}, 'egg-box'-like structures are proposed to become cross-linked to form multi-stacked poly-guluronate (G) segments. Poly-mannuronate (M) and mixed MG stretches are also proposed to be important for intermolecular chain entanglement.

3.2. Percolation theory

The critical scaling exponent (s') and gelation (C_o') concentration were determined according to the method by Yano et al. (1993), as shown in Fig. 3 for a gellan solution in the absence of added ions at 25 °C. Similar plots were observed for other gellan solutions and for κ-carrageenan and alginate polysaccharides in the absence and presence of added ions. Mean C_o' and s' values for all solutions are shown in Fig. 4. An individual degree of freedom contrast analysis found the interactions between the main effect contrasts (i.e. (1) no salts vs. salts or (2) K^+ vs. Ca^{2+}) and polymer A (i.e. gellan/alginate vs. κ-carrageenan) for C_o' data to be significant ($P<0.001$, Table 1), suggesting that the effects of salts were different for polymers with carboxyl and sulfate reactive groups. The critical gelation concentration was lower for gellan and alginate polymers with added Ca^{2+} than K^+, whereas C_o' was lower with added K^+ than Ca^{2+} for κ-carrageenan (Fig. 4a). The interactions between polymer B (i.e. gellan vs. alginate) and the main contrasts: no salts vs. salts ($P<0.001$) and K^+ vs. Ca^{2+} ($P<0.05$, Table 1) for C_o' data were found to be significant indicating that the effect of added salts on C_o' was different for the two polymers (Fig. 4a). Both polymers in the presence of salts had lower C_o' values than solutions without, although C_o' for gellan decreased further than with alginate. Similarly, C_o' decreased further in the presence of Ca^{2+} than K^+ for both polymers, a trend more pronounced with gellan (Fig. 4b).

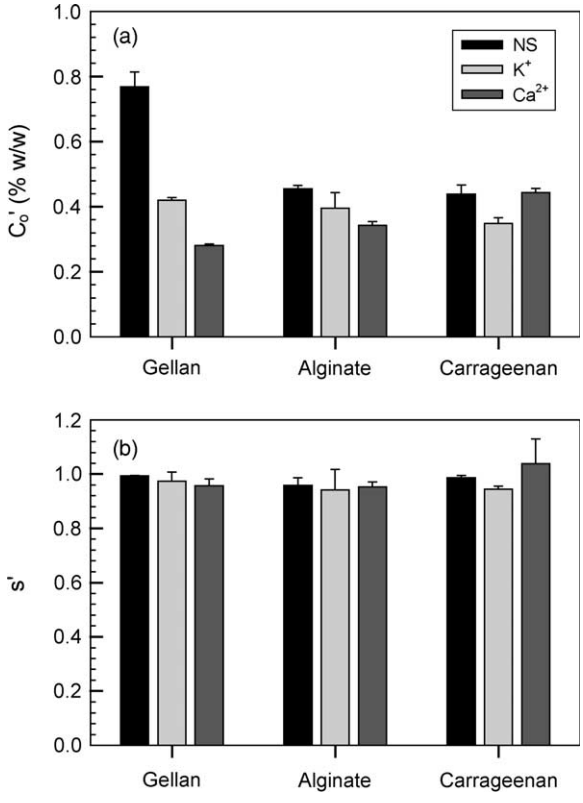

Fig. 4. The critical gelation concentration (C_o') (a) and scaling exponent (s') (b) as a function of polymer-type (i.e. gellan, alginate or κ-carrageenan) for solutions in the absence (NS) and presence of 0.5 mM K^+ or 0.25 mM Ca^{2+} ($n=2$). Error bars represent one standard deviation.

The critical gelation concentration for gellan and alginate solutions decreased with the addition of salts relative to solutions without, and decreased further with added Ca^{2+}. The decrease in C_o' with the addition of Ca^{2+} is proposed to reflect the formation of strong Ca^{2+} bridges between carboxyl sites, which allows a network to be formed at lower polymer concentrations. In the presence of K^+, charge screening was proposed to cause reduced intermolecular repulsion that enhanced polymer–polymer associations that may lead to a network being formed at lower concentrations than without added ions. For κ-carrageenan solutions, the addition of K^+ caused a modest decrease in C_o' relative to solutions without added ions, whereas there was no change with added Ca^{2+} (Fig. 4a). It is proposed that solutions with added K^+ form networks at lower concentrations than solutions without, due to increased charge screening and electrostatic attractive forces, as described earlier. With added Ca^{2+}, on the other hand, it is proposed that there was no effect on C_o' because of the large concentration of residual K^+ present.

An individual degree of freedom contrast analysis for s' data found the effects of the main contrasts (i.e. salt and polymer) and their interactions not to be significant ($P>0.05$, Table 1), indicating that gellan, alginate and κ-carrageenan have a similar overall aggregate structure. Mean s' values for all solutions are shown in Fig. 4b. However, it is noteworthy to mention that within the aggregate assemblage, junction zones will differ due to the inherent differences in polymer structure, concentration and ionic interactions. The percolation theory predicts a critical scaling exponent (s') ranging between 0.7 and 1.3, whereas the classical tree-like approximation predicts a constant s' value (i.e. $s'=0$). In the present study, mean s' values were estimated to range between 0.942 and 1.039 depending on the polymer and salts present (Fig. 4b), suggesting that s' values were similar to those predicted by the percolation model, where assemblages consisted of individual clusters and at C_o' an infinite cluster exists. Borchard and Lechtenfeld (2001) found 5% (w/w) gelatin in water to follow a percolation-type sol–gel transition finding an 's' value of ~0.7. Zheng, Zhang, Jiang, Zhang, and Wang (1996) found that alginate solutions in the presence of cupric ions behaved as individual clusters prior to the sol–gel transition finding an 's' value of 1.27.

3.3. Oscillatory shear rheometry

Frequency dependence of the viscoelastic storage (G') and loss (G'') moduli of a 0.7% (w/w) gellan solution in the absence of added ions were measured with controlled stress and oscillating magnetic bead rheometers to probe the bulk and local properties, respectively. However, the frequency spectra are not directly comparable because the controlled stress rheometer probes the sample on a micrometer length scale, whereas the oscillating bead rheometer shears on a nanometer level.

The frequency (ω) dependence of the bulk viscoelastic properties for a 0.7% (w/w) gellan solution in the absence of added ions is shown in Fig. 5. At $\omega < \sim 1.5$ Hz, flow behavior of G' and G'' were similar, scaling by a power-law function of $\omega^{0.52}$. Gellan chains were in the terminal region of the relaxation spectrum. At $\omega > \sim 1.5$ Hz, G' became greater than G'' as gellan polymer behavior entered the rubbery plateau zone of the viscoelastic spectrum. The two regions were separated by a terminal relaxation time (τ_R) of 1.32 s, as determined by $1/\omega$ at the crossover of G' with G''. The terminal region is dominated by very long relaxation mechanisms, where long-range conformational changes occur (i.e. motion over the gross polymer) (Ferry, 1980). In the plateau region, relaxation is intermediate between long- (i.e. terminal zone) and short-range (i.e. rubber–glass transition) motion (Ferry, 1980). Viscoelastic measurements of the bulk neglect small-scale heterogeneity that may arise because of the formation and aggregation of individual clusters. The log frequency responses of log G' and log G'' in the bulk is typical for an entangled polymer solution (Clark, 1992), which is consistent with a sample below C_o' (Fig. 4a).

Frequency dependence of the local viscoelastic behavior was determined separately for four embedded oscillating beads. Frequency spectra were described in terms of the relaxation and power-law behavior of the viscoelastic moduli (Fig. 6). At lower ω, moduli were within the rubbery plateau region where $G' > G''$, until G'' crossed over G' into the Rouse relaxation regime or rubber–glass transition at higher frequencies. The inverse frequency at the crossover corresponds to the relaxation time for the onset of entanglement constraints (τ_e) (Schmidt, Hinner, & Sackmann, 2000). This time varied from 0.67 to 2 s for the beads examined (Table 2). In the Rouse relaxation regime, G' and G'' scaled by a power-law function averaging $\omega^{0.46}$ and $\omega^{0.85}$, respectively (Table 2). The variation in both the scaling exponents and τ_e indicates that the sample is heterogeneous at the nanometer level. Interpretations from the oscillating bead rheometer should be taken with caution,

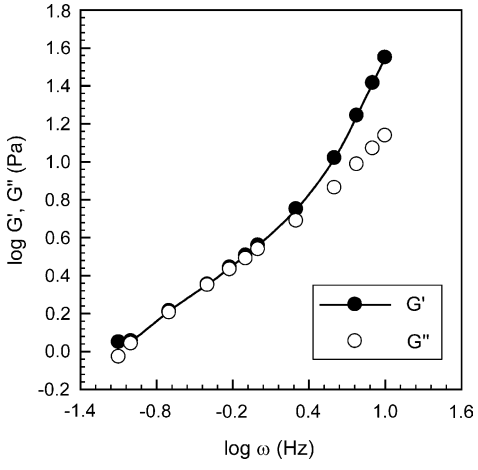

Fig. 5. Frequency (ω) dependence of G' and G'' for a 0.7% (w/w) gellan solution in the absence of added counterions, as measured using a controlled stress rheometer ($n=2$).

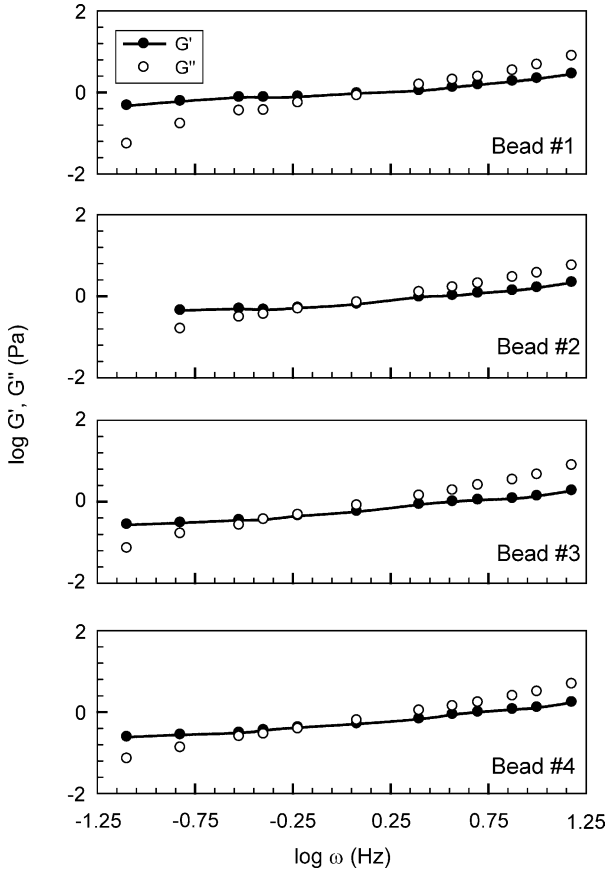

Fig. 6. Frequency (ω) dependence of G' and G'' for a 0.7% (w/w) gellan solution in the absence of added counterions, as measured using an oscillating magnetic bead rheometer.

Table 2
Power-law dependence of $G'(\omega)$ and $G''(\omega)$ in the Rouse relaxation regime and relaxation time at the onset of entanglement restraints (τ_e) for four different beads embedded within a 0.7% (w/w) gellan solution

Bead	τ_e (s)	$G'\alpha\omega^n$	$G''\alpha\omega^n$
1	0.67	0.52	0.89
2	1.26	0.45	0.81
3	2.00	0.43	0.88
4	1.26	0.43	0.80
Mean	1.30±0.54	0.46±0.04	0.85±0.05

however, because only four beads were measured within one sample, and the exact polymer distribution surrounding each bead is unknown.

4. Conclusion

Gellan, κ-carrageenan and alginate polysaccharides in the presence and absence of counterions had a similar overall mechanism of aggregation, irrespective of their different ordered domains and ion-mediated junction zones. Aggregation near the sol–gel transition followed the percolation theory, where individual clusters continually form until the critical gelation concentration, where an infinite cluster forms (i.e. gel). These clusters result in local heterogeneity within the sample matrix that is undetectable by rheological measurements of the bulk.

Acknowledgements

Financial assistance was provided by the Natural Sciences and Engineering Research Council of Canada. Special thanks to Drs E. Sackmann and M. Keller for their technical support while using the oscillating magnetic bead rheometer.

References

Anderson, N. S., Campbell, J. W., Harding, M. M., Rees, D. A., & Samuel, J. W. B. (1969). X-ray diffraction studies of polysaccharide sulphates: double helix model for κ- and ι-carrageenans. *Journal of Molecular Biology*, *45*, 85–99.

Arbabi, S., & Sahimi, M. (1990). Critical properties of viscoelasticity of gels and elastic percolation networks. *Physical Review Letters*, *65*, 725–728.

Borchard, W., & Lechtenfeld, M. (2001). Time dependent properties of thermoreversible gels. *Material Research Innovation*, *4*, 381–387.

Broderix, K., Löwe, H., Müller, P., & Zippelius, A. (2000). Critical dynamics of gelation. *Physical Review E*, *63*, 1–17.

Chandrasekaran, R., & Radha, A. (1995). Molecular architectures and functional properties of gellan gum and related polysaccharides. *Trends in Food Science and Technology*, *6*, 143–147.

Chandrasekaran, R., Radha, A., & Thailambal, V. G. (1992). Roles of potassium ions, acetyl and L-glyceryl groups in native gellan double helix: an X-ray study. *Carbohydrate Research*, *224*, 1–17.

Clark, A. H. (1992). Gels and gelling. In H. G. Schwartzberg, & R. W. Hartel (Eds.), *Physical chemistry of foods* (pp. 263–306). New York: Marcel Dekker.

Croguennoc, P., Meunier, V., Durand, D., & Nicolai, T. (2000). Characterization of semi dilute κ-carrageenan solutions. *Macromolecules*, *33*, 7471–7474.

de Gennes, P.-G. (1979). *Scaling concepts in polymer physics*. New York: Cornell University Press.

Del Gado, E., de Arcangelus, L., & Coniglio, A. (2002). Critical dynamics at the sol–gel transition. *Physica A*, *304*, 93–102.

Doner, L. W., & Douds, D. D. (1995). Purification of commercial gellan to monovalent cation salts results in acute modification of solution and gel-forming properties. *Carbohydrate Research*, *273*, 225–233.

Ferry, J. D. (1980). *Viscoelastic properties of polymers*. New York: Wiley.

Harding, S. E. (1998). Dilute solution viscometry of food biopolymers. In S. E. Hill, D. A. Ledward, & J. R. Mitchell (Eds.), *Functional properties of food macromolecules.* (2nd ed.). (pp. 1–49). Gaithersburg: Aspen Publishers.

Harding, S. E., Day, K., Dhami, R., & Lowe, P. M. (1997). Further observations on the size, shape and hydration of kappa-carrageenan in dilute solution. *Carbohydrate Polymers*, *32*, 81–87.

Ikeda, T., Tokita, M., Tsutsumi, A., & Hikichi, K. (1989). Critical elasticity of gelatin gel. *Japanese Journal of Applied Physics*, *28*, 1639–1643.

Jampen, S., Britt, I. J., & Tung, M. A. (2000). Gellan polymer solution properties: dilute and concentrated regimes. *Food Research International*, *33*, 579–586.

Jansson, P. E., Lindberg, B., & Sandford, P. A. (1983). Structural studies of gellan gum, an exocellular polysaccharide elaborated by *Pseudomonas elodea*. *Carbohydrate Research*, *124*, 135–139.

Keller, M., Schilling, J., & Sackmann, E. (2001). Oscillatory magnetic bead rheometer for complex fluid microrheometry. *Review of Scientific Instruments*, *72*, 3626–3634.

Lahaye, M. (2001). Chemistry and physico-chemistry of phycocolloids. *Cahiers de Biologie Marine*, *42*, 137–157.

Li, J. C. R. (1964). *Statistical inference I*. Ann Arbor: Edwards Brothers Inc.

Mao, R., Tang, J., & Swanson, B. G. (1999). Gelling temperatures of gellan solutions as affected by citrate buffers. *Journal of Food Science*, *64*, 648–652.

Meunier, V., Nicolai, T., & Durand, D. (2000). Structure and kinetics of aggregating κ-carrageenan studied by light scattering. *Macromolecules*, *33*, 2497–2504.

Morris, E. R., Rees, D. A., & Robinson, G. (1980). Cation-specific aggregation of carrageenan helices: domain model of polymer gel structure. *Journal of Molecular Biology*, *138*, 349–362.

Morris, V. J. (1986). Gelation of polysaccharides. In J. R. Mitchell, & D. A. Ledward (Eds.), *Functional properties of food macromolecules* (pp. 121–170). New York: Elsevier.

Morris, V. J. (1995). Bacterial polysaccharides. In A. M. Stephen (Ed.), *Food polysaccharides and their applications* (pp. 341–375). New York: Marcel Dekker.

Morris, V. J. (1998). Gelation of polysaccharides. In S. E. Hill, J. R. Mitchell, & D. A. Ledward (Eds.), *Functional properties of food macromolecules.* (2nd ed.). (pp. 143–226). New York: Elsevier.

Narsimhan, G. (1992). Emulsions. In H. G. Schwartzberg, & R. W. Hartel (Eds.), *Physical chemistry of foods* (pp. 307–386). New York: Marcel Dekker.

Nickerson, M. T., Paulson, A. T., & Speers, R. A. (2003). Rheological properties of dilute gellan solutions: effect of calcium ions and temperature on pre-gel formation. *Food Hydrocolloids*, *17*, 577–583.

te Nijenhuis, K. (1997). *Thermoreversible networks*. New York: Springer.

Robinson, G., Manning, C. E., & Morris, E. R. (1991). Conformation and physical properties of the bacterial polysaccharides gellan, welan, and rhamsan. In E. Dickinson (Ed.), *Food polymers, gels and colloids. No 82. Proceedings of the Royal Society of Chemistry International Symposium at Norwick, UK*.

Sanderson, G. R., & Clark, R. C. (1983). Laboratory-produced microbial polysaccharide has many potential food applications as a gelling, stabilizing, and texturing agent. *Food Technology*, *37*(4), 63–70.

Schmidt, F. G., Hinner, B., & Sackmann, E. (2000). Microrheometry underestimates the values of the viscoelastic moduli in measurements on F-actin solutions compared to macrorheometry. *Physical Review E*, *61*, 5646–5653.

Smidsrød, O., & Grasdalen, H. (1982). Some physical properties of carrageenan in solution and gel state. *Carbohydrate Polymers*, *2*, 270–272.

Stauffer, D., Coniglio, A., & Adam, M. (1982). Gelation and critical phenomena. *Advances in Polymer Science*, *44*, 103–158.

Steffe, J. F. (1996). *Rheological methods in food processing engineering* (2nd ed.). East Lansing: Freeman Press.

Tang, J., Tung, M. A., & Zeng, Y. (1995). Mechanical properties of gellan gels in relation to divalent cations. *Journal of Food Science*, *60*, 748–752.

Tang, J., Tung, M. A., & Zheng, Y. (1997a). Gelling temperature of gellan solutions containing calcium ions. *Journal of Food Science*, *62*, 276–280.

Tang, J., Tung, M. A., & Zheng, Y. (1997b). Gelling properties of gellan solutions containing monovalent and divalent cations. *Journal of Food Science*, *62*, 688–692.

Tempel, M., Isenberg, G., & Sackmann, E. (1996). Temperature-induced sol–gel transition and microgel formation in α-actinin cross-linked actin networks: a rheological study. *Physical Review E*, *54*, 1802–1810.

Thành, T. T. T., Yuguchi, Y., Mimura, M., Yasunaga, H., Takano, R., Urkawa, H., & Kajiwara, K. (2002). Molecular characteristics and gelling properties of carrageenan family, 1: preparation of novel carrageenans and their dilute solution properties. *Macromolecular Chemical Physics*, *203*, 15–23.

Tung, M. A., & Paulson, A. T. (1995). Rheological concepts for probing ingredient interactions in food systems. In A. G. Gaonkar (Ed.), *Ingredient interactions: effects on food quality* (pp. 45–83). New York: Marcel Dekker.

Ueda, K., Itoh, M., Matsuzaki, Y., Ochiai, H., & Imamura, A. (1998). Observation of the molecular weight change during the helix-coil transition of κ-carrageenan measured by the SEC-LALLS method. *Macromolecules*, *31*, 675–680.

Watase, M., & Nishinari, K. (1993). Effect of potassium on the rheological and thermal properties of gellan gum gels. *Food Hydrocolloids*, *7*, 449–456.

Weast, R. C. (1975). *Handbook of chemistry and physics.* (56th ed.). Cleveland: CRC Press.

Yano, T., Kumagai, H., Fujii, T., & Inukai, T. (1993). Concentration dependence of mechanical properties of polyacrylamide near the sol–gel transition point. *Bioscience, Biotechnology and Biochemistry*, *57*, 528–531.

Zheng, H. Z., Zhang, Q., Jiang, K., Zhang, H., & Wang, J. (1996). Critical behavior of viscosity for alginate solutions near the gelation threshold induced by cupric ions. *Journal of Chemical Physics*, *105*, 7746–7752.

Ziemann, F., Rädler, J., & Sackmann, E. (1994). Local measurements of viscoelastic moduli of entanglement actin networks using an oscillatory magnetic bead micro-rheometer. *Biophysical Journal*, *66*, 2210–2216.